Journal of Structural Integrity and Maintenance

ISSN: 2470-5314 (Print) 2470-5322 (Online) Journal homepage: https://www.tandfonline.com/loi/tstr20

Loss impact factors for lifetime seismic loss assessment of steel concentrically braced frames designed to EC8

John Hickey & Brian Broderick

JOURNAL OF STRUCTURAL INTEGRITY AND MAINTENANCE
2019, VOL. 4, NO. 3, 110–122
https://doi.org/10.1080/24705314.2019.1622186

Loss impact factors for lifetime seismic loss assessment of steel concentrically braced frames designed to EC8

John Hickey and Brian Broderick

Department of Civil, Structural & Environmental Engineering, Trinity College Dublin, Dublin, Ireland

ABSTRACT

This study employs multiple earthquake time-history response simulations, and the FEMA P-58 performance assessment methodology to evaluate the influence of key design parameters on the lifetime seismic repair costs incurred by case study concentrically braced frames (CBFs) designed to Eurocode 8. The parameters considered include structural mass, stiffness (natural period) and ductility (behaviour factor). A new factor termed the Loss Impact Factor (*LIF*), is used to quantify the influence of each of these parameters on lifetime costs. Under dissipative seismic design principles, bracing members in CBFs may behave inelastically under infrequent, high-intensity earthquakes. Larger values of the design behaviour factor, *q*, selected by the structural engineer result in higher ductility demands during these earthquakes, but also reduce the design seismic action, leading to smaller, lighter and more flexible structural members. Hence, variations in one parameter necessarily influence the others, as well as initial construction cost. The variation in expected lifetime seismic repair costs with respect to each of these parameters, which is less clear, is the subject of this paper. Costs are shown to reduce with increased structural mass, stiffness and initial cost, with the impact of the latter two parameters generally increasing with both seismic hazard and frame height.

KEYWORDS

Concentrically braced frame; behaviour factor; lifetime performance assessment; non-linear time history analysis; loss impact factor

Introduction

During an earthquake, buildings designed in accordance with modern seismic design codes are unlikely to suffer collapse (MacRae, Clifton, Bruneau, Kanvinde, & Gardiner, 2015; Okazaki, Lignos, Midorikawa, Ricles, & Love, 2013; Saatcioglu et al., 2013); however, significant structural and non-structural damage, and consequent losses, may still be experienced (Miranda, Mosqueda, Retamales, & Pekcan, 2012). As a result, increased attention is being placed on performance-based design strategies that attempt to achieve specified performance targets for a range of potential earthquake scenarios.

In order to examine a particular building design, seismic performance assessment methodologies have been developed to determine the probable values of different performance measures, such as repair costs or downtime. For a given earthquake scenario, the process of performance assessment typically involves conducting structural analysis to predict building response, assessing the likely amount of resultant damage and determining the probable consequences of that damage. Expected annual, and subsequently lifetime, performance measures can then be calculated by numerically integrating performance measures for a series of earthquake scenarios over all possible values of ground motion intensity.

The FEMA P-58 methodology (FEMA, 2012a) is a storey-based building-specific performance estimation methodology. The technical basis for the methodology is the so-called PEER (Pacific Earthquake Engineering Research Centre) framework, which is largely based in the work of Cornell and Krawinkler (2000) and has been further refined by Ramirez and Miranda (2012). To implement the FEMA P-58 methodology, multiple non-linear time history analysis (NLTHA) is performed at various ground motion intensity levels allowing Engineering Demand Parameters or *EDP*s, at each storey to be calculated. These *EDP*s are then used to calculate probable damage to various components of the building and subsequent consequences. Peak inter-storey drift and peak floor acceleration are the *EDP*s normally used to calculate damage; damage to structural elements, and some non-structural components is calculated based on the inter-storey drift with damage to other non-structural components being dependent on floor acceleration. The Performance Assessment Calculation Tool, known as PACT (FEMA, 2012b), has been developed to implement the methodology, using a list of damageable building components, known as a abuilding performance model, and *EDPs* to calculate performance measures of interest.

In conventional earthquake engineering practice, structures are typically designed to behave inelastically under large seismic loads. This is because for building frames, elastic behaviour requires significant forces to be resisted, necessitating the use of large, and expensive, structural members and connections. More efficient dissipative design can be achieved by allowing elements of the structure to yield under large, infrequent ground motions. In CBFs, this is done by allowing bracing members to yield in tension and buckle in compression, thereby utilising the ductility capacity of the braces to reduce the force and acceleration demands to acceptable levels.

In Eurocode 8 (CEN, 2004) based design, dissipative behaviour can be accounted for through the use of a single global behaviour factor, *q*, which can be expressed as:

$$q = \frac{F_{el}}{F_y} \tag{1}$$

CONTACT John Hickey hickeyj2@tcd.ie

where F_{el} is the peak seismic force that would develop in a Single Degree of Freedom (SDOF) system behaving linear elastically, and F_y is the yield strength of this SDOF system.

In design, selecting higher q values increases the degree of inelasticity likely to be experienced by the structure, however, the seismic forces to be resisted are reduced; hence as long as dissipative zones possess sufficient ductility to accommodate the increased plastic deformation, using higher q values allows the designer to select smaller, and consequently less expensive, structural members and connections. Furthermore, allowing structures to yield results in energy dissipation and reduced floor acceleration demands. EC8 specifies a maximum behaviour factor of 4 for CBFs with high ductility braces.

This paper assesses the extent to which the choice of behaviour factor impacts on the seismic performance of CBF structures. This is done by examining the expected lifetime losses suffered by a series of case study CBFs designed using different behaviour factors. For this study lifetime losses include costs incurred due to repair of structural and non-structural components and building demolition and are calculated using PACT. However, losses due to business downtime, injuries or fatalities are not considered.

Furthermore, varying the behaviour factor leads to variation in other parameters of interest. The selection of smaller sections leads to reduced structural mass, initial construction cost, and once material strength is kept constant, structural stiffness. Therefore, it is also possible to examine how expected losses vary with each of these parameters. From a design perspective, the paper explores the ability of the structural engineer to limit lifetime losses, while from an economic viewpoint it allows the potential saving in repair costs over a building's lifetime associated with an increased initial investment to be evaluated.

Procedure

Case study buildings

For this study, two sites, one in Oakland, California (37.803°, −122.287°) and one in Seattle, Washington (47.609, −122.334°) were selected as case study sites. The site in Oakland, which has previously been used in a number of previous studies (Baker, Lin, Shahi, & Jayaram, 2011; Terzic, Mahin, & Comerio, 2014), has a severe seismic hazard, whereas the design hazard at the Seattle is in line with more moderate values found in Europe. Sites in the US, as opposed to Europe, were selected because more comprehensive seismic information is available from the US Geological Survey (United States Geological Survey, 2008, 2014) than any European equivalent, something which is especially relevant for the Multiple Stripe Analysis approach to ground motion record selection described later.

A series of two, five and ten storey CBFs, as illustrated in Figure 1 and detailed in Tables 1–4, were designed in accordance with Eurocode 3 (CEN, 2005) and Eurocode 8 using behaviour factors between 1 and 5. Buildings were designed to be square in plan with seismic resistance provided by perimeter braced frames. For each frame, bay widths and storey heights were kept constant at 6 m and 3.6 m, respectively, except in the 10 storey frames where braced bay widths were halved, as can be seen in Figure 1. The frames were initially designed for gravity loading according to Eurocode 3 (CEN, 2005), with unfactored dead and live loads of 3 kN/m^2 and 3.3 kN/m^2 applied at each floor level and 2.6 kN/m^2 and 0.6 kN/m^2 at the roof level.

Subsequently, the seismic design was carried out in accordance with Eurocode 8. The USGS hazard application (United States Geological Survey, 2014) was used to obtain the 10% in 50 year peak ground acceleration for Type A ground at the sites, 0.5g in Oakland and 0.3g in Seattle, and these values were used as the reference peak ground acceleration, a_g, values to compute the Eurocode 8 design spectrum. The Type 1 design spectrum was used for both sites given the magnitudes of the earthquakes that contribute most to the seismic hazard.

The design actions to be resisted by the structural members were calculated through elastic analyses using the Eurocode 8 lateral force method for regular structures. The lateral resistance of the structure was assumed to be provided by the tension diagonals only. Based on the results of this analysis, the columns, which are UK Universal Column sections, and beams, UK Universal Beam sections, were capacity designed to resist the combination of gravity, and seismic actions stipulated by Eurocode 8, with member sizes kept constant at each level.

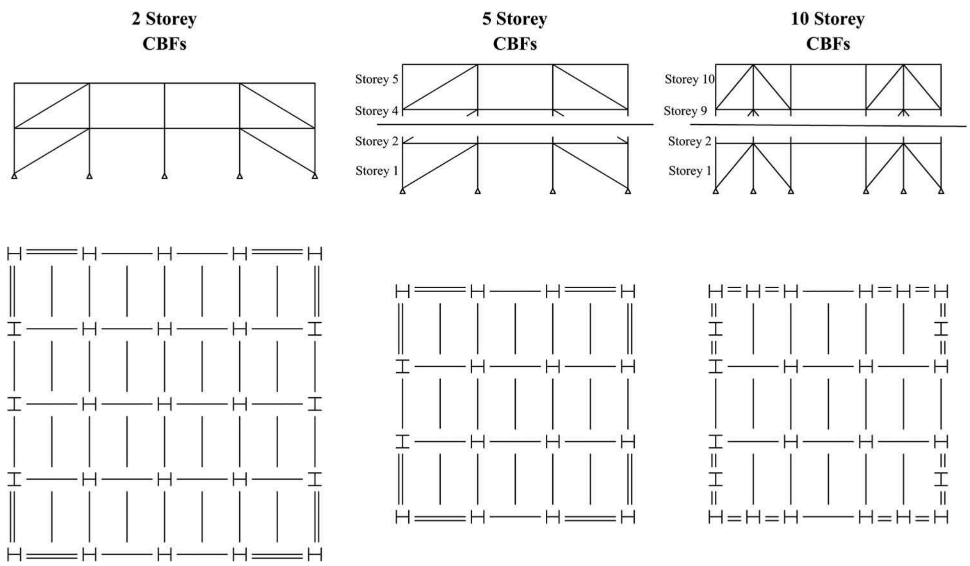

Figure 1. Illustration of case study CBFs.

Table 1. Details of case study frames; showing the influence of the behaviour factor, q, on the mass of steel required and the fundamental structural period, T_1.

		Oakland site; $a_g = 0.5g$		Seattle site; $a_g = 0.3g$	
No. of Stories	q	Mass of Steel (Mg)	T_1 (s)	Mass of Steel (Mg)	T_1 (s)
2	1	91.4	0.12	70.2	0.15
2	2	70.6	0.16	41.2	0.22
2	3	58.8	0.20	38.0	0.25
2	4	44.8	0.23	35.8	0.28
2	5	41.2	0.24	35.5	0.29
5	1	223.7	0.22	131.9	0.27
5	2	170.5	0.26	113.5	0.32
5	3	138.5	0.31	87.0	0.38
5	4	114.3	0.35	64.9	0.44
5	5	98.4	0.36	64.7	0.45
10	2	376.4	0.51	295.1	0.59
10	3	308.0	0.60	222.2	0.71
10	4	241.2	0.70	178.5	0.82

The bracing members, which were either rectangular or square hollow sections, were designed to resist axial forces due to the seismic design actions. The EC8 non-dimensional slenderness limitations and overstrength differential criteria were obeyed in the brace design procedure.

The majority of structural members were designed with an assumed yield strength of 355 N/mm^2; however, in a number of cases with lower behaviour factors, it was necessary to employ a yield strength of 460 N/mm^2 in non-dissipative members to fulfil capacity design criteria whilst maintaining a constant structural configuration. The Eurocode 8 deformation checks for second-order effects and damage limitation requirements were also performed as part of the design process, but as is the case for many CBF structures due to their high stiffness, these did not impact any of the designs.

Table 2. Details of beam (UKB), column (UKC) and brace (SHS or RHS) sections sizes for the 2 storey CBFs.

	Oakland Site; $a_g = 0.5g$			Seattle Site; $a_g = 0.3g$		
Level	Beam	Column	Brace	Beam	Column	Brace
		$q = 1$			$q = 1$	
2	305x165x40	305x305x198	300x200x12	305x165x40	305x305x137	140x140x12.5
1	533x312x182	305x305x198	500x300x12	457x191x106	305x305x137	300x200x12
		$q = 2$			$q = 2$	
2	305x165x40	254x254x132	140x140x10	305x165x40	203x203x86	120x120x6.3
1	457x191x89	254x254x132	250x150x12.5	305x127x48	203x203x86	140x140x10
		$q = 3$			$q = 3$	
2	305x165x40	254x254x132	140x140x6.3	305x165x40	203x203x71	120x120x5
1	406x178x60	254x254x132	200x120x10	305x165x40	203x203x71	140x140x6.3
		$q = 4$			$q = 4$	
2	305x165x40	254x254x107	140x140x5	305x165x40	203x203x60	120x120x4
1	305x165x40	254x254x107	140x140x8	305x165x40	203x203x60	140x140x5
		$q = 5$			$q = 5$	
2	305x165x40	254x254x89	120x120x5	305x165x40	203x203x60	120x120x4
1	305x165x40	254x254x89	140x140x6.3	305x165x40	203x203x60	120x120x5

Table 3. Details of beam (UKB), column (UKC) and brace (SHS or RHS) sections sizes for the 5 storey CBFs.

	Oakland Site; $a_g = 0.5g$			Seattle Site; $a_g = 0.3g$		
Level	Beam	Column	Brace	Beam	Column	Brace
		$q = 1$			$q = 1$	
5	610x305x238	203x203x71	200x150x8	457x191x106	203x203x46	140x140x7.1
4	610x305x238	305x305x137	300x200x12.5	457x191x106	254x254x89	250x150x12
3	610x305x238	356x406x340	450x250x12	457x191x106	356x368x202	300x200x12.5
2	610x305x238	356x406x340	500x300x12.5	457x191x106	356x368x202	400x200x12
1	610x305x238	356x406x467	500x300x16	457x191x106	356x406x287	500x300x10
		$q = 2$			$q = 2$	
5	457x191x133	203x203x71	120x120x7.1	406x178x67	203x203x46	120x120x5
4	457x191x133	305x305x198	250x150x10	406x178x67	203x203x86	200x120x10
3	457x191x133	305x305x198	300x200x12	406x178x67	305x305x198	250x150x10
2	457x191x133	356x406x340	500x300x8	406x178x67	305x305x198	250x150x12
1	457x191x133	356x406x340	400x200x12	406x178x67	305x305x240	300x200x10
		$q = 3$			$q = 3$	
5	406x178x85	203x203x60	120x120x5	305x165x46	152x152x51	120x120x4
4	406x178x85	305x305x158	140x140x8.8	305x165x46	203x203x60	200x120x6
3	406x178x85	305x305x158	140x140x12.5	305x165x46	254x254x167	140x140x8.8
2	406x178x85	356x406x287	250x150x12	305x165x46	254x254x167	250x150x8
1	406x178x85	356x406x287	250x150x12	305x165x46	305x305x198	250x150x8
		$q = 4$			$q = 4$	
5	356x171x57	203x203x60	120x120x4	305x165x40	152x152x44	150x100x3
4	356x171x57	305x305x137	140x140x6.3	305x165x40	203x203x46	120x120x6.3
3	356x171x57	305x305x137	140x140x8.8	305x165x40	254x254x89	140x140x7.1
2	356x171x57	356x406x235	200x120x10	305x165x40	254x254x89	140x140x8.8
1	356x171x57	356x406x235	140x140x12.5	305x165x40	305x305x118	140x140x8.8
		$q = 5$			$q = 5$	
5	305x127x48	203x203x60	120x120x4	305x165x40	152x152x37	100x100x3.6
4	305x127x48	305x305x118	140x140x6.3	305x165x40	152x152x51	100x100x7.1
3	305x127x48	305x305x118	200x120x8	305x165x40	254x254x89	140x140x7.1
2	305x127x48	356x368x202	200x120x10	305x165x40	254x254x89	140x140x8
1	305x127x48	356x368x202	140x140x12.5	305x165x40	254x254x107	140x140x8.8

Table 4. Details of beam (UKB), column (UKC) and brace (SHS or RHS) sections sizes for the 10 storey CBFs.

	Oakland Site; a_g = 0.5g			Seattle Site; a_g = 0.3g		
Level	Beam	Column	Level	Beam	Column	Level
		q = 2			q = 2	
10	356x127x33	152x152x44	100x100x5	356x127x33	152x152x37	80x80x4
9	356x127x33	203x203x86	200x100x8	356x127x33	203x203x86	100x100x7.1
8	406x140x46	305x305x118	400x200x6	356x127x33	203x203x113	120x120x8.8
7	406x178x60	305x305x198	250x150x12	305x165x40	254x254x167	180x100x10
6	457x152x74	356x406x287	450x250x8	305x165x40	305x305x198	140x140x12.5
5	406x178x85	356x406x393	500x300x8	305x165x46	305x305x283	250x150x10
4	457x191x98	356x406x467	400x200x12	356x171x51	356x406x340	250x150x10
3	457x191x98	356x406x551	450x250x10	356x171x57	356x406x467	250x150x12
2	457x191x106	356x406x677	500x300x10	356x171x67	356x406x551	250x150x12
1	457x191x106	356x406x818	500x300x10	406x178x60	356x406x634	250x150x12.5
		q = 3			q = 3	
10	305x165x40	203x203x60	80x80x4	356x127x33	152x152x30	80x80x3
9	305x165x40	203x203x71	90x90x8.8	356x127x33	203x203x46	120x80x5
8	305x165x40	305x305x137	140x140x8	356x127x33	203x203x86	90x90x8
7	305x165x40	305x305x158	200x120x10	305x165x40	203x203x127	120x120x8
6	305x165x46	356x406x235	400x200x6	305x165x40	254x254x167	180x100x8
5	305x165x54	356x406x287	300x200x8	305x165x40	305x305x198	200x120x8
4	356x171x57	356x406x393	250x150x12	305x165x40	356x406x235	140x140x10
3	406x178x60	356x406x467	250x150x12.5	305x165x40	356x406x287	200x100x10
2	356x171x67	356x406x551	300x200x10	305x165x40	356x406x340	200x120x10
1	356x171x67	356x406x634	300x200x10	305x165x40	356x406x467	200x120x10
		q = 4			q = 4	
10	305x165x40	152x152x30	80x80x3	356x127x33	152x152x30	70x70x3
9	305x165x40	203x203x52	90x90x6.3	356x127x33	152x152x51	100x100x4
8	305x165x40	254x254x89	140x80x8	356x127x33	203x203x60	90x90x7.1
7	305x165x40	254x254x132	180x100x8	305x165x40	203x203x100	140x80x8
6	305x165x40	356x368x153	200x120x8	305x165x40	254x254x107	120x120x8
5	305x165x40	356x406x235	200x100x10	305x165x40	305x305x137	140x140x8
4	305x127x48	356x406x287	140x140x12.5	305x165x40	356x368x177	180x80x10
3	305x127x48	356x406x340	140x140x12.5	305x165x40	356x368x202	200x120x8
2	356x171x45	356x406x393	250x150x10	305x165x40	356x406x235	180x100x10
1	305x165x54	356x406x467	250x150x10	305x165x40	356x406x287	140x140x10

Structural modelling

To carry out NLTHA, the frames were modelled in OpenSees (McKenna, 2011). Individual planar models were created for both primary response directions, with one component of the ground motion pair applied to the model representing one direction and the orthogonal component applied to the other model, in accordance with the PACT recommendations (FEMA, 2012b).

Following the recommendations of Uriz, Filippou, and Mahin (2008), the bracing elements were modelled using two force-based nonlinearBeamColumn elements with three integration points per element. An initial camber displacement of 0.1% of the brace length was employed at the midpoint in order to simulate buckling behaviour. The brace elements were discretised as illustrated in Figure 2(a). The beams and columns were also modelled using force-based nonlinearBeamColumn elements with three integration points and discretized fibre sections. Column and beam buckling were not modelled explicitly in the structural models; however, the axial forces in the columns and beams were monitored in all simulations and never exceeded the Eurocode 3 design buckling load, $N_{b,Rd}$. Therefore, column and beam buckling were deemed to not occur. Non-linear rotational spring elements, with initial rotational stiffness and yield moment calculated according to the expressions proposed by Hsiao, Lehman, and Roeder (2012), were employed at the brace end point to simulate the end restraint imposed on the braces by the gusset plates. Rigid elements were used to model the remainder of the gusset plates and the sections of the beams and columns in the region of the connection, as illustrated in Figure 2(b). The Steel02 material, which represents the Giuffre-Menegotto-Pinto model, was used for all non-linear components. As illustrated in Figure 3, a fictitious leaning column element (Geschwindner, 2002) was included in order to account for second-order effects due to the gravity loads from parts of the building not included in the OpenSees models. For all analysis 3% Raleigh damping proportional to the mass and tangent stiffness matrix at the first and third modes was applied. Stiffness proportional damping was not applied to any rigid or leaning column elements.

Selection of ground motion records

Through a sensitivity analysis (Hickey, 2018), it was shown that carrying out NLTHA at eight intensity levels using 10 two-component ground motion records is sufficient to calculate lifetime performance metrics using the FEMA P-58 methodology. Analysis was carried for ground motion intensities with 2% (known as the Maximum Credible Earthquake or MCE, intensity level), 5% 10% (Design Level Earthquake, DLE), 15%, 30%, 50% (Service Level Earthquake, SLE), 70% and 95% probabilities of exceedance in 50 years, meaning a wide range of potential earthquake scenarios are considered in lifetime performance assessment. In order to select ground motion records for NLTHA, a Multiple Stripe Analysis (MSA) approach was adopted. MSA involves selecting different sets of ground motion records at each ground motion intensity level considered (Baker, 2013). This is in contrast to more frequently employed Incremental Dynamic Analysis (IDA) procedures, where the same set of progressively scaled records is used for all intensities. The MSA approach captures the variations in expected characteristics of ground motions at different intensities meaning that the records selected,

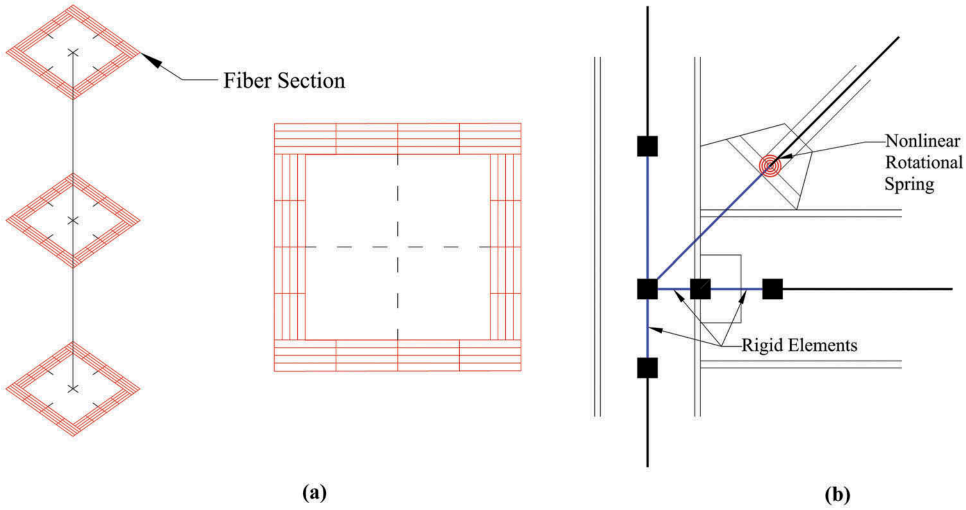

Figure 2. (a) Distributed plasticity square hollow section element with fibre cross-section and three integration points; b) model of gusset plate connection as per Hsiao et al. (2012).

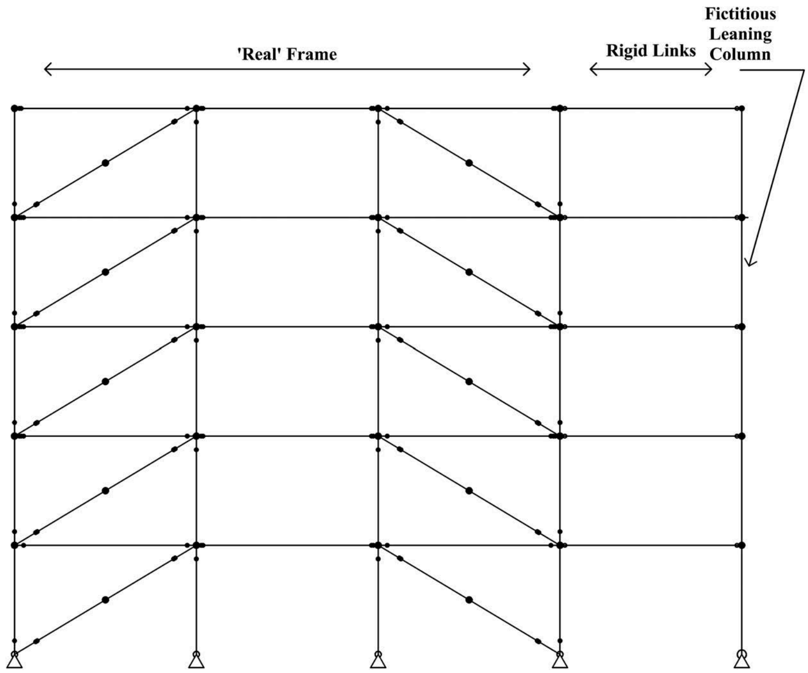

Figure 3. OpenSees model of 5 storey CBF.

and consequently the calculated structural response, will be hazard consistent.

Ground motion selection and modification for MSA involves the development of a target response spectrum representative of the seismic hazard at each intensity level of interest and then selecting and scaling ground motion records to match this target. The conditional spectrum (CS) (Baker, 2010) was used as the target spectrum in this study based on the recommendations of Lin, Haselton, and Baker (2013). In that study, the impact on calculated *EDP* values of selecting ground motion records to match the various potential target spectra was assessed, and the CS was recommended for performance assessment type procedures.

The CS is calculated based on a conditioning period, T^*, which is typically the fundamental period of the structure being examined. Ideally, each frame would be analysed with ground motion records selected to match a spectrum conditioned on its fundamental period; however, this would mean employing different sets of records for each frame. However, it has been shown (Lin et al., 2013) that when using the CS, probabilistically weighted structural analysis results are relatively insensitive to the choice of conditioning period. It was therefore considered acceptable to use the mean fundamental period for each frame height at each site as the conditioning period for developing the target spectrum. This ensured that frames designed with different behaviour factors were subjected to the same set of ground motion records, allowing the impact of the behaviour factor to be fairly assessed.

The procedure for selecting ground motion records firstly involved seismic hazard deaggregation, which was performed for the case study sites using the USGS tool (United States Geological Survey, 2008). Then, using the results from this, MATLAB code, available online (https://web.stanford.edu/~bakerjw/gm_selection.html) (Jayaram, Lin, & Baker, 2011) was used to calculate the appropriate CS and scale and select appropriate two-component ground motion records from the PEER NGA database (Chiou, Darragh, Gregor, & Silva, 2008). This process was carried out for both case study sites, meaning separate sets of records were selected for each. The difference in seismicity between the two sites is accounted for by the use of the CS, which is site-specific (Baker, 2013). Figure 4 shows the records selected for the 2% in 50, 10% in 50 and 50% in 50 years (i.e. the MCE, DLE and SLE) probability of exceedance intensity levels at each site for the 2 storey CBFs. The conditioning period, T^*, which is 0.2 s for these frames at the Oakland site and 0.235 s for the Seattle site, is also marked. Similar sets of records, with different conditioning periods, were used for the analysis of the 5 and 10 storey frames.

Results

Structural analysis – EDPs

Figures 5 and 6 show the seismic response analysis results obtained for the 5 storey CBFs by applying the selected ground motions to the OpenSees structural models. The median values of the maximum inter-storey drift and floor acceleration results recorded in the 10-time history analyses at each intensity level are presented. As expected, as the earthquake intensity (represented by the spectral acceleration at the conditioning period, $S_a(T^*)$), value to which the ground motion records are scaled increases, the *EDPs* of interest increase accordingly.

The peak inter-storey drift increases consistently with the design behaviour factor, which is as expected given that increasing q results in a more flexible structure. At the higher intensity levels, the peak floor acceleration response of the dissipative (q = 4 or q = 5) frames is reduced compared to the non-dissipative designs due to yielding. At lower intensity levels, when the frames behave elastically, accelerations display less sensitivity to the behaviour factor than inter-storey drifts. This is attributable to the fact that the periods of the frames analysed here tend to lie within the constant acceleration region of the spectrum and therefore changing the behaviour factor, and consequently the structural period, doesn't greatly affect the acceleration response in the elastic region. Similar trends were observed for the 2 and 10 storey CBFs analysed, but are not shown here for brevity.

Expected repair costs

Losses examined here incorporate costs incurred due to repair of structural and non-structural building components as well as losses due to building demolition. The probability of building demolition was calculated in PACT using the building repair fragility function proposed in FEMA P-58

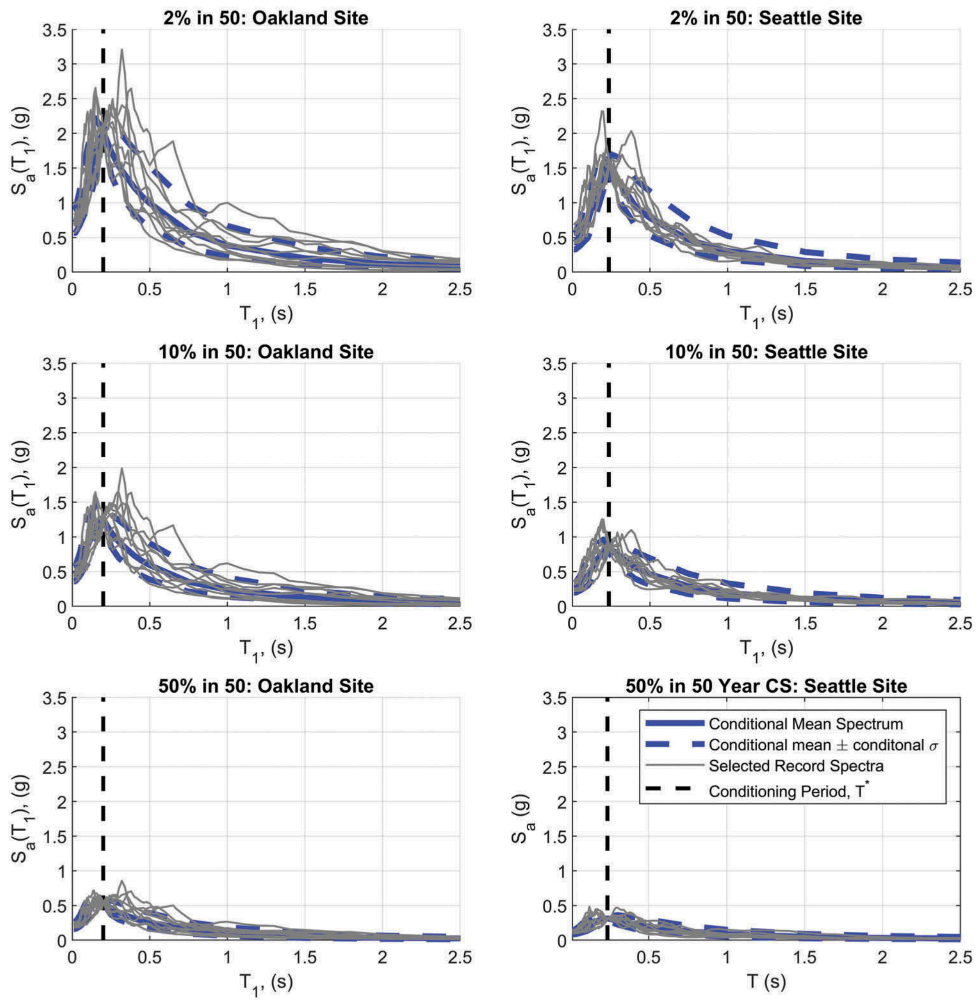

Figure 4. Conditional spectra and selected ground motion records for the 2%, 10% and 50% in 50-year intensity levels for the two storey CBFs at the two case study sites.

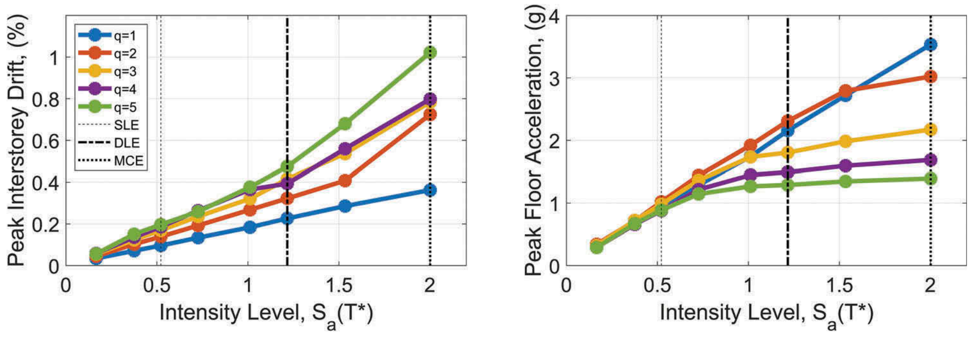

Figure 5. Median peak inter-storey drift and peak floor acceleration response for the 5 storey CBFs at the Oakland site.

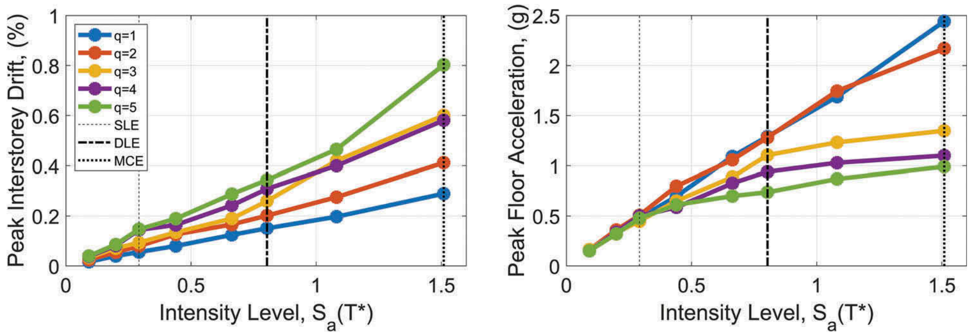

Figure 6. Median peak inter-storey drift and peak floor acceleration response for the 5 storey CBFs at the Seattle site.

(FEMA, 2012a), which has a median residual drift value of 1.0% and a log-normal standard deviation of 0.3.

Structural collapse was not considered in the calculation of repair costs. This is because it is challenging to identify collapse accurately with structural models that do not contain any deteriorating components, particularly when a limited number of ground motions is used. More importantly, however, collapse is typically expected to occur at inter-storey drifts in the range of 3–5% (Hsiao, Lehman, & Roeder, 2013), whereas the peak inter-storey drift recorded in this study is 2.53%. Therefore, the contribution of collapse to lifetime losses is expected to be negligible.

The *EDPs* recorded in structural analysis, namely maximum inter-storey drift, and floor acceleration at each level, as well as peak residual inter-storey drift, were used as the inputs for loss assessment, which was carried out in PACT. The structural components incorporated in this loss analysis are listed in Table 5, which also provides a brief description of each damage state, as well as the median and distribution terms that define the fragility functions. The quantities of structural components used in loss analysis at each floor level, which dictates the repair cost, were selected on a floor by floor basis based on member sizes in each case study frame. All fragility and consequence functions for structural components are those specified in FEMA P-58 (FEMA, 2012b).

The buildings were assumed to be office buildings, and the type and quantities of non-structural components used in the loss analysis were obtained using the normative quantities recommended by FEMA P-58 (FEMA, 2012b). The non-structural components considered in the loss analysis are listed in Table 6, which also gives the median and distribution terms that define the fragility functions for each damage state. All non-structural components are selected

Table 5. Details of structural components included in the PACT building model for performance assessment for case study buildings, including the median, μ, in % inter-storey drift, and lognormal standard deviation, β, of fragility functions used in damage assessment.

		Fragility Parameters		
PACT ID	Component	Damage State	μ	*B*
B1031.011a/	Column Base Plate	Crack Initiation	4%	0.4
B1031.011b/	(*a* for column < 150 pounds/ft, *b* for column 150–300 pounds/ft and *c* for column > 150 pounds/ft)	Crack Propagation	7%	0.4
B1031.011c		Fracture	10%	0.4
B1031.021a/	Welded Column Splice	Crack initiation	4%	0.4
B1031.021b/	(*a* for column < 150 pounds/ft, *b* for column 150–300 pounds/ft and *c* for column > 150 pounds/ft)	Crack Propagation	7%	0.4
B1031.021c		Fracture	10%	0.4
B1031.001	Shear Tab Connection	Yielding	4%	0.4
		Partial tear	8%	0.4
		Separation	11%	0.4
B1033.022a/	Brace & gusset plate	Buckling (< depth of brace)	0.37%	0.3
B1033.022b/	(*a* for brace < 40 pounds/ft, *b* for brace 41–99 pounds/ft and *c* for brace > 100 pounds/ft)	Buckling (> depth of brace)	0.75%	0.25
B1033.022c		Buckling (> twice depth of brace)	1.45%	0.25
		Fracture	1.99%	0.35

Table 6. Non-structural components included in the PACT building model for performance assessment for case study buildings (*included at ground floor only, **included at roof level only), including median, μ in percentage inter-storey drift for the drift sensitive components and in g for the acceleration sensitive components, and log-normal standard deviation, β, of fragility function used in damage assessment.

PACT ID	Component	Quantity per floor level (2 storey buildings)	Quantity per floor level (5 & 10 storey buildings)	Unit	Fragility Parameters μ (DS1, DS2, DS3)	Fragility Parameters B (DS1, DS2, DS3)
			Drift Sensitive Non-Structural Components			
B2022.002	Curtain Walls	1860	1046.4	Square Feet (SF)	2.1% 2.4%	0.45 0.45
C1011.001a	Gypsum Partition Walls	620	349	Linear Feet (LF)	0.21% 0.71% 1.2%	0.6 0.45 0.45
C2011.001a	Prefabricated steel stair	1	1	Unit(s)	2.5% 3.7% 4.8%	0.6 0.6 0.45
			Acceleration Sensitive Non-Structural Components			
C3027.002	Raised Access Floor	4650	2616	SF	1.5g	0.4
C3032.003d	Suspended Ceiling (Area>232m^2)	5580	3140	SF	0.35g 0.55g 0.8g	0.4 0.4 0.4
C3034.002	Independent Pendant Lighting	93	52	Unit(s)	1.5g	0.4
D2021.013a	Cold Water Piping	90	50	LF	2.25g 4.1g	0.5 0.5
D2021.013b	Cold Water Piping Bracing	90	50	LF	1.5g 2.25g	0.5 0.5
D2022.013a	Hot Water Piping (Small)	520	290	LF	0.55g 1.1g	0.5 0.5
D2022.013b	Hot Water Bracing (Small)	520	290	LF	2.25g	0.5
D2022.023a	Hot Water Piping (Large)	180	100	LF	2.25g 4.1g	0.5 0.5
D2022.023b	Hot Water Bracing (Large)	180	100	LF	1.5g 2.25g	0.5 0.5
D2031/013b	Sanitary Pipe Bracing	360	200	LF	2.25g	0.5
D3041.011c	HVAC Galvanized Sheet Metal Ducting < 6 sq. ft in cross sectional area	470	260	LF	1.5g 2.25g	0.4 0.4
D3041.012c	HVAC Galvanized Sheet Metal Ducting > 6 sq. ft cross sectional area	120	70	LF	3.75g 4.5g	0.4 0.4
D3041.031b	HVAC Drops/Diffusers	55.8	31	Unit(s)	1.3g	0.4
D3041.041b	Variable Air Volume (VAV) box	43.4	24	Unit(s)	1.9g	0.4
D4011.063a	Fire Sprinkler Drop	56	31	Unit(s)	0.55g 1.3g	0.4 0.4
D5012.023a/D5012.023c	Low Voltage Switchgear (a for anchorage only damaged (Seattle), c for both anchorage and equipment (Oakland))	1	1	Unit(s)	1.9125g (Oakland) 1.1475g (Seattle)	0.5
D5012.013b/ D5012.013d	Motor Control Center* (b for anchorage only damaged (Seattle), d for both anchorage and equipment (Oakland))	1	1 (5 storey) 2 (10 storey)	Unit(s) Unit(s)	0.765g (Oakland) 0.459g (Seattle)	0.5
D1014.011	Traction Elevator *	1	1	Unit(s)	0.39g	0.45
B3011.011	Concrete tile roof**	1674	942	SF	1.1g 1.4g	0.4 0.4
D3031.013c	Chiller**	1	1	Unit(s)	1.9125g (Oakland) 1.1475g (Seattle)	0.4
D3031.023c	Cooling Tower**	1	1 (5 storey) 2 (10 storey)	Unit(s)	1.9125g (Oakland) 1.1475g (Seattle)	0.4
D3052.013c	Air Handling Unit**	2	4 (5 storey) 8 (10 storey)	Unit(s)	1.9125g (Oakland) 1.1475g (Seattle)	0.4

for high seismicity sites. All consequence functions, and where possible the fragility functions, for the non-structural components used in loss analysis are those specified in FEMA P-58.

Fragility functions are not directly available in PACT for some elements. Following the recommendation of FEMA P-58, fragility functions for stairs with a seismic joint are developed by adding an assumed design drift of 2% to the median value of the FEMA P-58 fragility functions for stairs without a seismic joint. Fragility functions for anchored MEP components are developed using the recommendations for anchored equipment in FEMA P-58, with design floor acceleration calculated in accordance with Eurocode 8. Finally, it should be noted that suspended ceilings are conservatively assumed to run continuously over partitions, as opposed to being independent within each room at a floor level. This assumption can have a significant impact on the calculation of lifetime acceleration sensitive repair costs.

Losses were calculated for each earthquake intensity level examined. Expected Annual Losses (*EAL*) are calculated by integrating the losses at each intensity level over the hazard curve for the site in question. This gives a higher weighting to more frequently occurring, lower intensity earthquakes. Therefore, these events are of greater importance for lifetime loss assessment than the less frequent, higher intensity events. The present value (*PV*) of lifetime repair costs is then calculated from the *EALs* using Equation (2) (Wen & Kang, 2001):

$$PV = EAL \times \frac{1 - e^{-rt}}{r} \tag{2}$$

where r is a discount factor, taken here as 3%, that accounts for inflation by converting costs incurred due to future earthquakes into present values, and t is the lifetime of the building, taken here as 50 years. This method of calculating the present value of lifetime costs is widely used in losses assessment studies (for example in Macedo and Castro (2017) or using a similar method in Hwang and Lignos (2017)), and assumes the building is repaired to its original condition after each earthquake occurrence. Any potential building deterioration over time is not accounted for within the formulation. The expected annual losses and the present value of expected lifetime losses for each CBF are given in Table 7.

Figure 7 shows the present value of the estimated 50-year financial losses as a percentage of the initial cost for each building type. Initial costs are estimates as \$250/ft^2, plus an additional cost of \$4000 per tonne of extra steel used as the behaviour factor is reduced (Terzic et al., 2014).

It can be seen that the seismic repair costs incurred are lowest for the q = 1 frames (or q = 2 for the 10 storey frames where a q = 1 frame was not analysed) and increases as the behaviour factor is increased. The expected losses increase with the number of stories due to the increased inter-storey drift in the taller, more flexible frames.

Figure 7 also shows the breakdown of financial losses between drift and acceleration sensitive components, as well as the contribution of demolition costs. As can be seen from Tables 5 and 6, drift sensitive components include the structural system as well as some non-structural elements such as curtain walls, while acceleration sensitive components are non-structural elements such as service ducts, raised access floors and suspended ceilings. For the two and five storey CBFs, repairs to acceleration sensitive components are generally the major contributor to overall costs. However, drift resultant costs become more significant as the number of stories is increased, contributing to a greater extent than acceleration dependant losses to the overall estimated repair costs for 10 storey CBFs. Costs related to building demolition due to excessive residual drift were shown to be very small (less than 0.4% of initial costs) in all cases. The minor contribution of residual drift-related losses to lifetime costs for CBFs has been noted elsewhere (Hwang & Lignos, 2017), illustrating one of the benefits of the inherent stiffness of braced frame structures.

Drift sensitive repairs grow with the behaviour factor to a much greater extent than acceleration dependant costs. This trend can be explained by considering the results of structural analysis discussed previously. Peak inter-storey drift was shown to increase with the behaviour factor, in contrast to peak floor acceleration, which was relatively insensitive to q at the lower intensity levels, which are given greater weighting in the lifetime performance calculation. Consequently, the behaviour factor impacts on drift sensitive repair costs to a much greater extent. Given that drift dependant costs become more significant with frame height, the benefit of reducing behaviour factor, and limiting drift dependent losses, becomes more pronounced as the number of stories is increased.

Repair costs are greater for the Oakland site compared to the Seattle site, which makes sense given the respective seismic hazards. This is particularly evident for the 10 storey CBFs, as the hazard reduction between the two sites is greatest at higher structural periods. The difference in repair costs between the two sites is primarily attributable to the extent of the damage suffered at frequently occurring intensity levels (50% in 50 years and below). The greater intensity of these ground motions at the Oakland site results in greater damage and subsequent repairs, particularly to non-structural, acceleration sensitive components. As these repair costs are associated with more frequent earthquakes, their contribution to the lifetime repair cost calculation is heavily weighted and therefore influential on the final result.

Table 7. Expected annual losses and present value of lifetime losses for each case study CBF.

		Oakland site; a_g = 0.5g		Seattle site; a_g = 0.3g	
No. of Stories	q	EAL (\$)	PV (\$)	EAL (\$)	PV (\$)
2	1	8,781	225,922	4,511	116,063
2	2	11,728	301,752	6,356	163,539
2	3	14,171	364,616	8,590	221,011
2	4	14,348	369,169	9,783	251,705
2	5	14,604	375,746	9,414	242,215
5	1	13,722	353,073	6,793	174,787
5	2	17,728	456,138	7,818	201,159
5	3	19,170	493,238	8,787	226,087
5	4	22,191	570,977	10,033	258,140
5	5	22,401	576,371	10,494	270,002
10	2	49,144	1,264,460	17,707	455,589
10	3	64,685	1,664,317	23,183	596,492
10	4	88,111	2,267,078	27,456	706,424

Loss impact factor – LIF

In order to further understand the impact of the behaviour factor on calculated lifetime repair costs, a linear trend line is fitted to the total expected costs for each frame height and site. This concept is illustrated by the black lines in Figure 8.

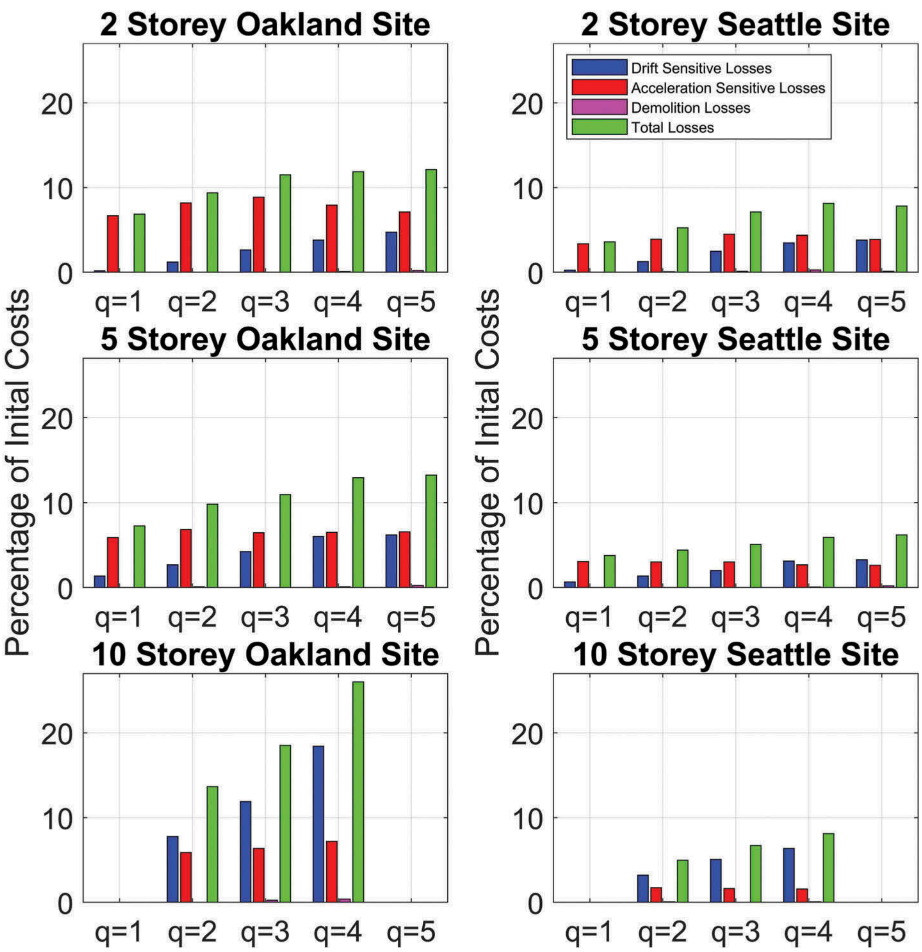

Figure 7. Present value of expected 50-year losses as a percentage of initial costs broken down into contributions from drift sensitive losses, acceleration sensitive losses and losses due to building demolition.

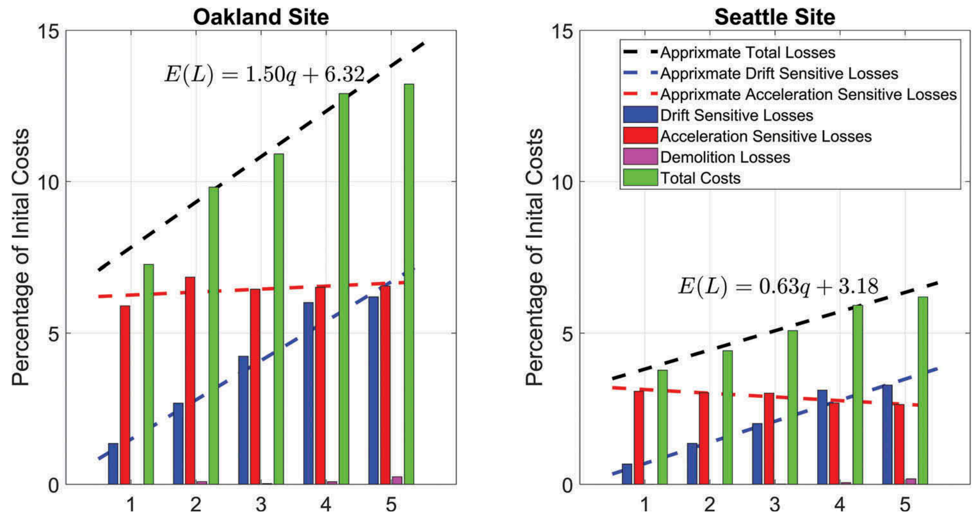

Figure 8. Illustration of the concept of LIF_q, the black dotted lines, LIF_{q_Drift}, the blue dotted lines, and LIF_{q_Acc}, the red-dotted lines, for 5 storey CBFs.

The slope of this line, which is termed the Loss Impact Factor or LIF_q, numerically quantifies the influence of q on the expected losses; a greater LIF_q value means that q has a larger impact on expected losses. The LIF_q values obtained for each set of case study buildings are presented in Table 8. The value of the intercept, c, is also given in Table 8, such that the present value of expected repair costs can be approximated as:

$$E(L) = LIF_q \times q + c \tag{3}$$

From Table 8, it can be seen that the LIF_q generally increases with both frame height and seismic hazard. This indicates that the impact of q on expected losses becomes more important as frame height and seismic hazard are increased. The value of the LIF_q indicates what percentage of the initial costs are saved by reducing q by 1; for example for the 10 storey frames, savings

Table 8. LIF_q values for the case study CBFs.

	Oakland Site		Seattle Site	
No. of Stories	LIF_q (%initial/q)	c	LIF_q (%initial/q)	c
2	1.30	6.43	1.13	2.97
5	1.50	6.32	0.63	3.18
10	6.17	0.87	1.57	1.88

of over 6% of the initial cost for the Oakland site can be achieved if the designer reduces the behaviour factor by 1. For the 2 and 5 storey frames, this saving is in the order of 1 to 1.5% of the initial cost.

LIF_q values were also calculated for the drift sensitive and acceleration sensitive losses. These are termed LIF_{q_Drift} and LIF_{q_Acc} respectively and are the slopes of the blue and red lines in Figure 8. The values of LIF_{q_Drift} and LIF_{q_Acc} for each case study scenario are given in Table 9. The LIF_{q_Drift} values are reasonably similar to the LIF_q values given in Table 8, reflecting the fact that the increases in losses with q are primarily due to an increase in drift dependent losses. The LIF_{q_Drift} values are consistently greater than the LIF_{q_Acc} values; showing that q has a greater impact on drift sensitive loss than acceleration sensitive losses. The LIF_{q_Acc} values are generally positive but close to zero, meaning that acceleration sensitive losses generally increase minimally with q. However, for the 5 and 10 storey CBFs at the Seattle site, the LIF_{q_Acc} values are negative, showing that acceleration dependent losses tend to decrease slightly with q in these scenarios.

Impact of fundamental period and structural mass – LIF_T & LIF_M

It is possible to extend the concept of the Loss Impact Factor to any design parameter in order to approximately examine how it impacts expected losses. Table 10 gives values for *LIF* with respect to the mass of steel and the fundamental period, termed LIF_M and LIF_T respectively. Clearly, these parameters are related to q, as both structural mass and period are functions of the design behaviour factor; however it is still relevant to examine the respective *LIFs*, firstly to understand the extent of the potential savings that can be made through design alterations and secondly to appreciate the universal applicability of the *LIF* concept to any parameter.

The LIF_M values presented are negative, indicating that losses reduce as the mass of steel used in the structure is increased. The magnitude of the LIF_M values ranges from 0.03 to 0.12 percent of initial cost per Mg of steel. On average, lifetime losses equal to approximately 0.07% of initial costs are saved by increasing the weight of the structure by 1 Mg, or, on a more relevant scale, increasing the weight of the structure by 50 Mg reduces lifetime repair costs by 3.5% of initial costs on average.

The positive LIF_T values indicate that increased fundamental period results in increased losses, or conversely, increased frame stiffness leads to reduced losses. The impact of the fundamental period on expected losses generally increases with seismic hazard. For the Seattle site, a design alteration that reduces the fundamental period by 0.1 s saves approximately 1.5% of initial cost in lifetime costs. The variation of LIF_T is more extreme for the Oakland site, with a 0.1 s reduction in T_1 leading to lifetime loss reductions of approximately 4.3%, 4.0% and almost 6.5% of initial costs for 2, 5 and 10 storey CBFs, respectively.

On a general level, examining the trends with respect to fundamental elastic period is relevant in the context of the development of seismic design code methods towards performance-based design procedures. When considering a specific structural form like CBFs, any alternative design process (e.g. displacement-based design methods like those proposed by Calvi and Sullivan (2009) or the alterations in brace overstrength limitations suggested by Brandonisio, Toreno, Grande, Mele, and De Luca (2012)), unless it involves the use of special devices like base isolation or damping devices, will at a fundamental level result in a modified frame with different strength and stiffness properties. For steel building frames, these two properties are closely linked, hence the variations in lifetime costs with design behaviour factor presented above reflect changes in both the lateral stiffness and lateral resistance of the CBF. Due to the high weighting of more frequent earthquakes in which frames behave elastically in the lifetime performance assessment procedure, the elastic response was observed to dominate expected lifetime losses. Therefore, for any change in the design process, its impact on lateral stiffness, and hence fundamental period is of greatest importance from a lifetime performance perspective. This means that the trends quantified by the LIF_T values can be used to examine the expected impact of any design alteration on lifetime losses. For example, the alternative brace overstrength rules for CBFs design proposed by Brandonisio et al. (2012) tend to result in frames with a longer structural period. The positive LIF_T values calculated in this study suggest that this would result in increased lifetime repair costs, the extent of which would depend on the seismic hazard.

Table 9. LIF_{q_Drift} and $LIFq_{\_Acc}$ values for the case study CBFs.

	Oakland Site		Seattle Site	
No. of Stories	LIF_{q_Drift} (%initial/q)	LIF_{q_Acc} (%initial/q)	LIF_{q_Drift} (%initial/q)	LIF_{q_Acc} (%initial/q)
2	1.17	0.07	0.93	0.15
5	1.30	0.10	0.70	−0.12
10	5.32	0.66	1.58	−0.08

Table 10. LIF_T and LIF_M values for the case study CBFs.

	Oakland Site		Seattle Site	
No. of Stories	LIF_M (%initial/Mg)	LIF_T (%initial/s)	LIF_M (%initial/Mg)	LIF_T (%initial/s)
2	−0.11	43.47	−0.12	33.35
5	−0.05	40.43	−0.03	13.04
10	−0.09	65.17	−0.03	13.68

Return on investment – $LIF_\$$

Finally, the *LIF* calculated with respect to the estimated initial cost, termed $LIF_\$$, is presented. This is calculated using dollar values, as opposed to percentages, for both expected losses and initial costs. This means that $LIF_\$$ is a measure of how effectively the extra money invested initially to reduce q is utilized on average across each of the behaviour factors examined. Therefore, $LIF_\$$ is a measure of the return on investment; an $LIF_\$$ value with a magnitude equal to 1 means that increasing the initial cost by \$1 results in lifetime loss savings of \$1. $LIF_\$$ magnitudes less than 1 means that increasing the initial cost by \$1 results in lifetime loss savings of less than \$1, while $LIF_\$$ magnitudes greater than 1 mean that increasing the initial cost by \$1 results in lifetime loss savings greater than \$1. Hence, an $LIF_\$$ magnitude greater than 1 implies that the initially more expensive frames with

Table 11. Return on Investment, $LIF_\$$, values for the case study CBFs.

	Oakland	Seattle
No. of Stories	$LIF_\$$ ($\$_{loss}/\$_{initalCost}$)	$LIF_\$$ ($\$_{loss}/\$_{initialCost}$)
2	−0.75	−0.86
5	−0.46	−0.33
10	−1.85	−0.53

lower ductility demands make the extra investment worthwhile, whereas the opposite is true for $LIF_\$$ magnitudes less than 1.

Table 11 presents the $LIF_\$$ values for the buildings analysed. Firstly, it can be seen that the $LIF_\$$ values are all negative, reflecting the negative correlation between initial costs and expected losses, i.e. repair costs are reduced as investment increases. It can be seen that for the 2 and 5 storey frames, and the 10 storey frame at the Seattle site, the magnitudes of the $LIF_\$$ values are less than 1, ranging from 0.33 to 0.75 \$/\$. This means that on average lifetime losses are reduced by \$0.33 to \$0.75 for every extra dollar spent initially. Clearly, this represents a poor return on investment, and indicates that for these scenarios employing highly dissipative designs, i.e. using behaviour factors of $q = 4$ or $q = 5$, is the best way to reduce total life costs. In contrast, for the 10 storey frames at the Oakland site the magnitude of the $LIF_\$$ value is 1.85; hence for every \$1 invested approximately \$1.85 are saved. This suggests that using initially more expensive, less-dissipative designs, i.e. $q = 2$ or less, is ultimately economically beneficial for taller frames at highly seismic sites.

Conclusions

Lifetime performance assessment was performed for a set of CBFs designed using behaviour factors ranging from 1 to 5. Performance was measured using estimated repair costs, which were calculated using the FEMA P-58 performance assessment methodology. The concept of a Loss Impact Factor (*LIF*) was introduced, allowing many of the key trends observed with respect to financial losses to be expressed quantitatively.

It was demonstrated that expected repair costs were minimised for the lowest behaviour factor used in design. For the 2 and 5 storey frames, losses resulting from damage to acceleration-sensitive non-structural components are generally the largest contributor to overall losses, with drift-induced damage being more significant for the 10 storey frames. The *LIF* values obtained demonstrate that reducing the behaviour factor limits drift sensitive losses, and as these become more significant with increasing frame flexibility, the impact of the behaviour factor on performance becomes more pronounced. Comparing severe and medium level seismic hazard sites, it was shown that lifetime losses are substantially greater for the severe seismic hazard site, primarily due to the increased damage suffered under frequently occurring seismic events.

On a more general level, the study demonstrates how performance assessment methodologies can be employed to improve and optimise structural design. The results indicate the extent to which inter-storey drift, and consequently damage and losses suffered by drift sensitive components, can be limited by increasing the stiffness of the structure, either indirectly through lowering the behaviour factor or through a focussed design alteration. In contrast, the designer appears to have little control over lifetime losses suffered by acceleration sensitive elements, at least for typical low and mid-rise CBFs that lie in the constant acceleration region of the spectrum.

Disclosure statement

No potential conflict of interest was reported by the authors.

References

Baker, J. W. (2010). Conditional mean spectrum: Tool for ground-motion selection. *Journal of Structural Engineering*, *137*(3), 322–331.

Baker, J. W. (2013). *Trade-offs in ground motion selection techniques for collapse assessment of structures*. Proceedings of Vienna Congress on Recent Advances in Earthquake Engineering & Structural Dynamics, Vienna, Paper Mo. 123.

Baker, J. W., Lin, T., Shahi, S. K., & Jayaram, N. (2011). New ground motion selection procedures and selected motions for the PEER transportation research program. *Peer Report*, *2011*, 3.

Brandonisio, G., Toreno, M., Grande, E., Mele, E., & De Luca, A. (2012). Seismic design of concentric braced frames. *Journal of Constructional Steel Research*, *78*, 22–37.

Calvi, G. M., & Sullivan, T. J. (2009). *A model code for the displacement-based seismic design of structures*. Pavia: IUSS Press.

CEN. (2004). *Eurocode 8 EN 1998-1:2004 Eurocode 8: Design of strucutres for earthquake resistance, part 1-1: General rules, seismic actions and rules for buildings*. Brussels: European Committee of Standardization.

CEN. (2005). *Eurocode 3 EN 1993-1-1:2005 Eurocode 3: Design of steel structures - Part 1-1: General rules and rules for buildings*. Brussels: European Committee of Standardization.

Chiou, B., Darragh, R., Gregor, N., & Silva, W. (2008). NGA project strong-motion database. *Earthquake Spectra*, *24*(1), 23–44.

Cornell, C. A., & Krawinkler, H. (2000). Progress and challenges in seismic performance assessment. *PEER newsletter*

FEMA. (2012a). *P 58-1 (2012) Seismic performance assessment of buildings (volume 1-Methodology)*. Washington, D.C.: Federal Emergency Management Agency.

FEMA. (2012b). *P 58-2 (2012) Seismic performance assessment of buildings (volume 2-Implemenation Guide)*. Washington, D.C.: Federal Emergency Management Agency.

Geschwindner, L. F. (2002). 2000 T.R. Higgins award paper - A practical look at frame analysis, stability and leaning columns. *Engineering Journal-American Institute of Steel Construction Inc*, *39*(4), 167–181.

Hickey, J. (2018). *Numerical & experimental investigation of the seismic performance of concentrically braced steel frame strucutres* (PhD thesis). Trinity College Dublin.

Hsiao, P. C., Lehman, D. E., & Roeder, C. W. (2013). Evaluation of the response modification coefficient and collapse potential of special concentrically braced frames. *Earthquake Engineering Structural Dynamics*, *42*(10), 1547–1564.

Hsiao, P.-C., Lehman, D. E., & Roeder, C. W. (2012). Improved analytical model for special concentrically braced frames. *Journal of Constructional Steel Research*, *73*, 80–94.

Hwang, S.-H., & Lignos, D. G. (2017). Effect of modeling assumptions on the earthquake-induced losses and collapse risk of steel-frame buildings with special concentrically braced frames. *Journal of Structural Engineering*, *143*(9), 04017116.

Jayaram, N., Lin, T., & Baker, J. W. (2011). A computationally efficient ground-motion selection algorithm for matching a target response spectrum mean and variance. *Earthquake Spectra*, *27*(3), 797–815.

Lin, T., Haselton, C. B., & Baker, J. W. (2013). Conditional spectrum-based ground motion selection. Part II: Intensity-based assessments and evaluation of alternative target spectra. *Earthquake Engineering & Structural Dynamics*, *42*(12), 1867–1884.

Macedo, L., & Castro, J. M. (2017). Earthquake loss assessment of steel moment-resisting frames designed according to EC8. *Ce/Papers*, *1*(2–3), 3801–3810.

MacRae, G., Clifton, G. C., Bruneau, M., Kanvinde, A., & Gardiner, S. (2015). Lessons from steel structures in Christchurch earthquakes. *Behaviour of Steel Structures in Seismic Areas STESSA*, *2015*, 1474–1481.

McKenna, F. (2011). OpenSees: A framework for earthquake engineering simulation. *Computing in Science & Engineering*, *13*(4), 58–66.

Miranda, E., Mosqueda, G., Retamales, R., & Pekcan, G. (2012). Performance of nonstructural components during the 27 February 2010 Chile earthquake. *Earthquake Spectra*, *28*(S1), S453–S471.

Okazaki, T., Lignos, D. G., Midorikawa, M., Ricles, J. M., & Love, J. (2013). Damage to steel buildings observed after the 2011 Tohoku-Oki earthquake. *Earthquake Spectra*, *29*(S1), S219–S243.

Ramirez, C. M., & Miranda, E. (2012). Significance of residual drifts in building earthquake loss estimation. *Earthquake Engineering & Structural Dynamics*, *41*(11), 1477–1493.

Saatcioglu, M., Tremblay, R., Mitchell, D., Ghobarah, A., Palermo, D., Simpson, R., & Hong, H. (2013). Performance of steel buildings and nonstructural elements during the 27 February 2010 Maule (Chile) Earthquake. *Canadian Journal of Civil Engineering*, *40*(8), 722–734.

Terzic, V., Mahin, S., & Comerio, M. (2014, Jan). *Life-cycle cost and performance comparisons of different code-compliant systems*. Northridge, CA, Northridge 20 Symposium.

United States Geological Survey. (2008). 2008 interactive deaggregations. Retrieved from http://geohazards.usgs.gov/deaggint/2008/

United States Geological Survey. (2014). Hazard curve application. Retrieved from http://geohazards.usgs.gov/hazardtool/application.php

Uriz, P., Filippou, F. C., & Mahin, S. A. (2008). Model for cyclic inelastic buckling of steel braces. *Journal of Structural Engineering*, *134*(4), 619–628.

Wen, Y.-K., & Kang, Y. (2001). Minimum building life-cycle cost design criteria. I: Methodology. *Journal of Structural Engineering*, *127*(3), 330–337.